Chapter 6

Applications of Direct AC-AC Converter

Contents

6.1 Introduction
6.2 Proposed switch mode power supply
6.3 Proposed converter PWM modulation
6.3.1 Rectifier mode of operation
6.3.2 Inverter mode of operation
6.4 Proposed switching modulation
6.5 Design Example
6.6 Input filter design
6.7 Simulation results
6.8 Experimental results
6.9 Applications of conventional Direct AC-AC converters for variable frequency wind turbine applications:
6.10 Implementation of proposed converter for control of DFIM for wind turbines
6.10.1 C_{rotor} control system
6.10.2 C_{grid} control system
6.11 Conclusion

Application of Direct AC-to-AC converters

6.1 Introduction

Modern telecommunication power systems require several rectifiers in parallel to obtain higher current DC output at -48 VDC [9], [20]-[22]. Commercially available telecom-rectifiers [23] employ AC to DC conversion stage with a boost converter, followed by a high frequency DC/DC converter to produce -48 VDC (see Fig. 6.1). This type of rectifier draws significant 5th and 7th harmonic currents resulting in near 35% total harmonic distortion (THD). In addition, the rectifier DC-link capacitor stage is bulky, contributes to weight and volume. Furthermore, the presence of multiple power conversion stages contributes to lower efficiency.

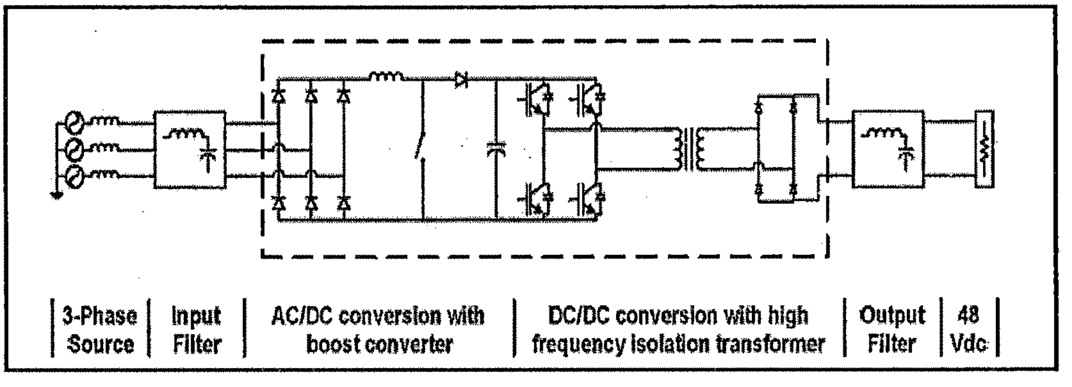

Fig. 6.1. Conventional telecommunication switch mode power supply.

In response to these concerns, this chapter proposes a digitally controlled switch mode power supply based on a matrix converter for telecommunication applications (Fig. 4.2). Matrix converter topology employs six bi-directional switches to convert lower frequency (60/50 Hz) three-phase input directly to a high frequency (10/20 kHz) single phase output. The output is then processed via an isolation transformer and rectified to -48 VDC. Digital control of the matrix converter stage ensures that the output voltage is regulated against load changes as well as input supply variations while maintaining sinusoidal input current shape at near unity power factor.

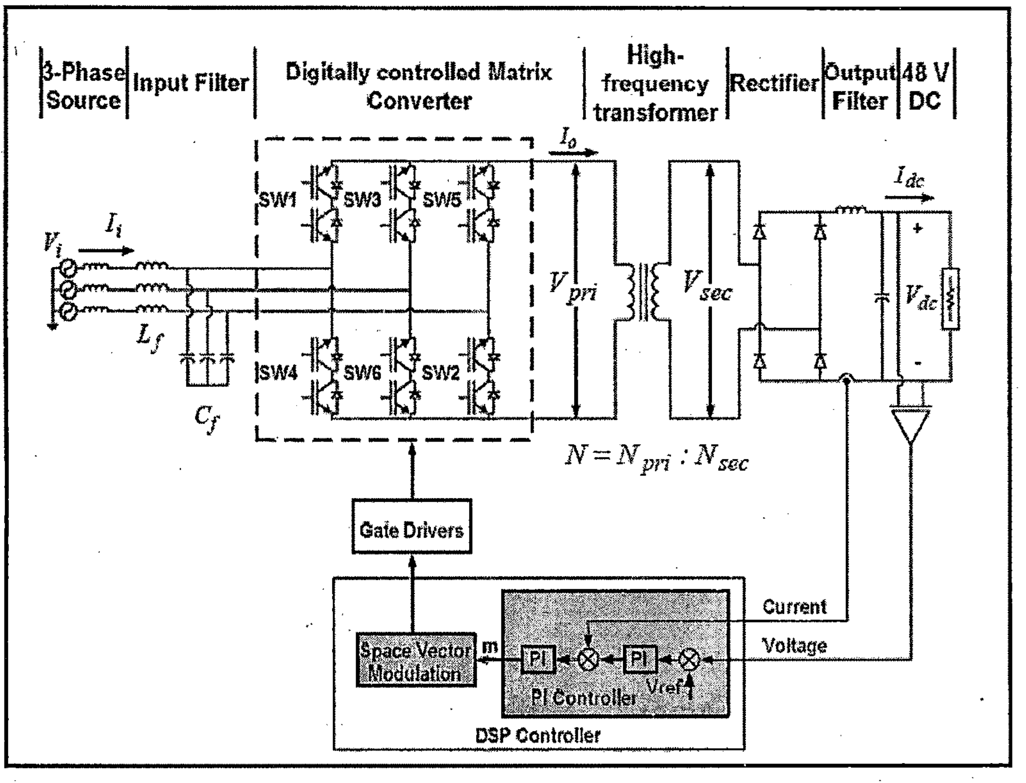

Fig.6.2. Proposed digitally controlled switch mode power supply based on matrix converter.

Advantages of the proposed topology are:

- No DC-link capacitor required.
- Capable of operation over a wide input voltage range.
- Low total harmonic distortion (THD) in line current.
- Proper switching modulation results in smaller input filter.
- Unity input power factor over a wide load range.
- Higher efficiency with increased power density.

- Digital control facilitates external communication; enable parallel operation of several stages and implementation of complex closed-loop control functions.

First section of this chapter presents a very prospective application of the proposed topology in the field of Telecom sector. The conceptual model analysis has been explained along with discussion on the modulation scheme is carried out. Initial trials are carried out and experimental results of a small capacity concept are presented.

6.2 Proposed switch mode power supply

The proposed digitally controlled switch mode power supply based on matrix converter is shown in Fig. 6.2. Matrix converter topology employs six bi-directional switches to convert lower frequency (60/50 Hz) three-phase input directly to a high frequency (10/20 kHz) single phase output. The output is then processed via an isolation transformer and rectified to -48 VDC. Digital control of the matrix converter stage ensures that the output voltage is regulated against load changes as well as input supply variations.

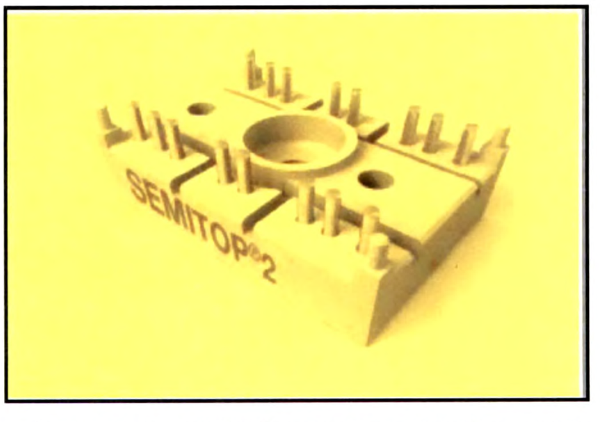

Fig. 6.3. Semikron make 2-IGBT switch module for matrix converter implementation

Matrix converter is a direct AC/AC converter and operates without a DC-link [25]. It has the advantage of bidirectional power flow, controllable input power factor, high reliability, and compact design. High operating frequency of the system allows the size and weight of the transformer to be reduced. In this topology, space vector modulation technique applied to a matrix converter is employed. For hardware implementation, a three-phase to three-phase matrix converter module based on 1200V IGBT introduced by EUPEC [24] is used (see Fig. 6.3).

6.3 Proposed converter PWM modulation

In the proposed topology a three-phase to single phase matrix converter (Fig. 6.4) using twelve IGBT switches is employed.

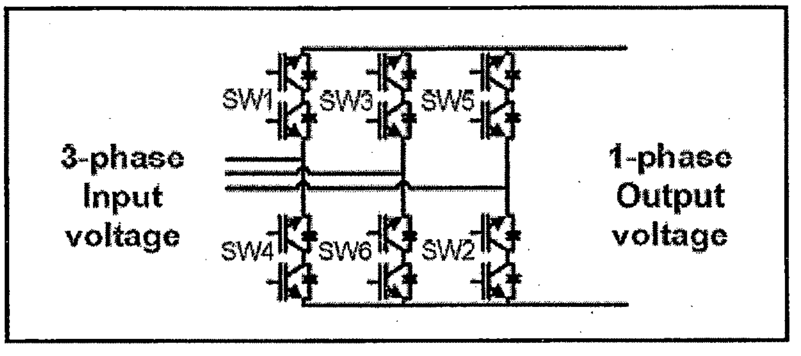

Fig. 6.4. A figure of three-phase to single phase matrix converter.

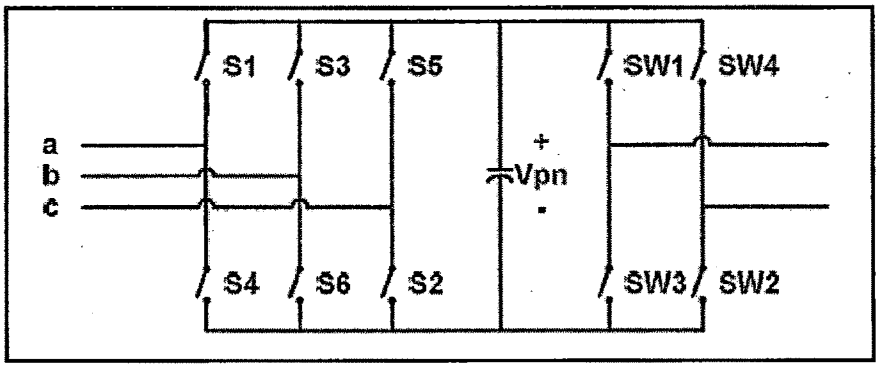

Fig. 6.5. Illustration of matrix converter operation.

The PWM modulation is divided to 2 modes, rectifier mode and inverter mode, respectively [26], [27]. Fig. 6.5 illustrates the modulation modes of matrix converter as traditional AC/DC/AC conversion system. Due to the absence of DC-link, V_{pn} is presented as a fictitious DC voltage for analysis purposes. The operation of the matrix converter can be expressed mathematically in a matrix formation. The fictitious DC voltage, V_{pn} , is derived from the rectifier mode of operation:

$$\boxed{V_{pn} = F_r * V_i} \tag{6.1}$$

where F_r is rectifier mode transfer function and $_iV$ is the input voltage vector. Matrix converter output voltage, V_o , is derived from the inverter mode of operation as follows:

$$\boxed{V_o = F_i * V_{pn}} \tag{6.2}$$

where F_i is the inverter mode transfer function. The line current I_i can be expressed in terms of rectifier and inverter mode transfer functions as:

$$\boxed{I_i = F_r^T * F_i^T * I_o} \tag{6.3}$$

The three-phase input voltage vector $_iV$ is given by,

$$\boxed{V_i = \begin{bmatrix} V_{an} \\ V_{bn} \\ V_{cn} \end{bmatrix} = \begin{bmatrix} V_m \sin(\omega_i t) \\ V_m \sin(\omega_i t - 120°) \\ V_m \sin(\omega_i t + 120°) \end{bmatrix}} \tag{6.4}$$

where V_m is amplitude of input voltage and ω_i is input angular frequency.

6.3.1 Rectifier mode of operation

As detailed in the earlier section, matrix converter analysis is simplified by separating the rectifier and inverter mode of operations. The objective of the rectifier mode of operation is to create a fictitious DC voltage $_{pn}V$ from input voltage and to maintain unity input power factor. Rectifier space vector hexagon is shown in Fig. 6.6.

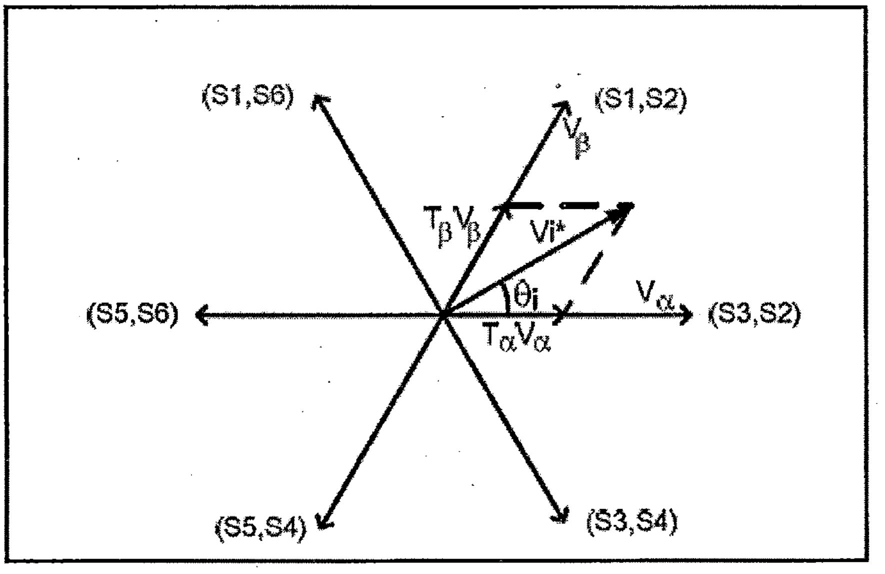

Fig. 6.6. Rectifier space vector hexagon.

The switching vectors in the hexagon in Fig. 6.6 are indicated by the switches from rectifier part in Fig. 6.5. The placement of space vector reference vector, V_i*, within one sector is defined by adjacent the switching vectors, V_α and V_β. The angle θ_i is angle of space vector reference vector. The duty cycles of the active switching vectors are calculated with rectifier mode modulation index, m_c.

$$\boxed{T_\alpha = m_c \sin\left(\frac{\pi}{3} - \theta_i\right)} \quad (6.6)$$

$$\boxed{T_\beta = m_c \sin(\theta_i)} \quad (6.7)$$

$$\boxed{T_o = 1 - T_\alpha - T_\beta} \quad (6.8)$$

Rectifier mode matrix, F_r, can be set up from switching functions S1 to S6 established by space vector method. Number of elements in F_r depends on the number of input phases.

$$\boxed{F_r = [F_{r1} \quad F_{r2} \quad F_{r3}]} \tag{6.9}$$

$$\boxed{F_{r1} = S_1 - S_4} \tag{6.10}$$

$$\boxed{F_{r2} = S_3 - S_6} \tag{6.11}$$

$$\boxed{F_{r3} = S_5 - S_2} \tag{6.12}$$

It can be stated that F_{r2} and F_{r3} are the same function as F_{r1} with phase shifting of -120° and +120°respectively.

6.3.2 Inverter mode of operation

The objective of this mode of operation is to generate a high frequency single phase output voltage. The operating frequency in this mode is the same as desired output frequency.

From the rectifier mode, fictitious DC voltage, V_{pn}, is found. It is used as the input of single phase inverter part in Fig. 6.5. Due to only one phase for the matrix converter output, the inverter mode matrix, F_i, has single element.

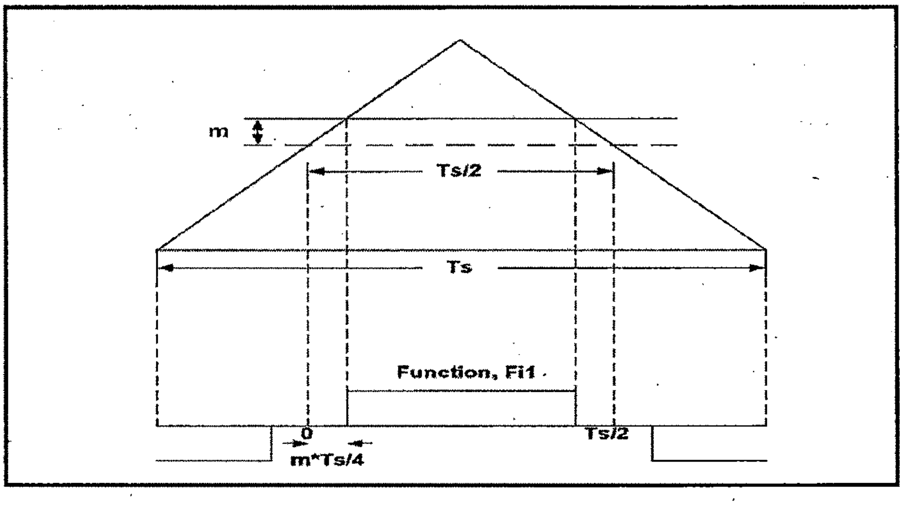

Fig. 6.7. Inverter mode switching function.

$$\boxed{F_i = [F_{i1}]} \tag{6.13}$$

$$\boxed{F_{i1} = SSW1 - SSW3 = SSW2 - SSW4} \qquad (6.14)$$

The switching function, F_{i1}, can be generated as shown in Fig. 6.7. The control signal, m_v, is varied to obtain desired matrix converter output voltage. The switching function can be expressed as:

6.4 Proposed switching modulation

From equation 4.1 and 4.2, it can be shown that matrix converter output can be found from:

Equation (4.18), the transfer function, TF, is representing the matrix converter switching function. Thus, switching function of matrix converter switches can be realized as follows.

$$\boxed{F_T = \begin{bmatrix} SSW_1 & SSW_3 \\ SSW_4 & SSW_2 \end{bmatrix} \times \begin{bmatrix} S_1 & S_3 & S_5 \\ S_4 & S_6 & S_2 \end{bmatrix}} \qquad (6.15)$$

$$\boxed{SW_1 = SSW_1 \times S_1 + SSW_3 \times S_4} \qquad (6.16)$$

$$\boxed{SW_2 = SSW_4 \times S_5 + SSW_3 \times S_2} \qquad (6.17)$$

$$\boxed{SW_3 = SSW_1 \times S_3 + SSW_3 \times S_6} \qquad (6.18)$$

$$\boxed{SW_4 = SSW_4 \times S_1 + SSW_2 \times S_4} \qquad (6.19)$$

$$\boxed{SW_5 = SSW_1 \times S_5 + SSW_3 \times S_2} \qquad (6.20)$$

$$\boxed{SW_1 = SSW_4 \times S_3 + SSW_2 \times S_6} \qquad (6.21)$$

Block diagram of the proposed matrix converter modulation is shown in Fig. 6.8. Each switch can be implemented with the logic gates as shown in Fig. 6.9.

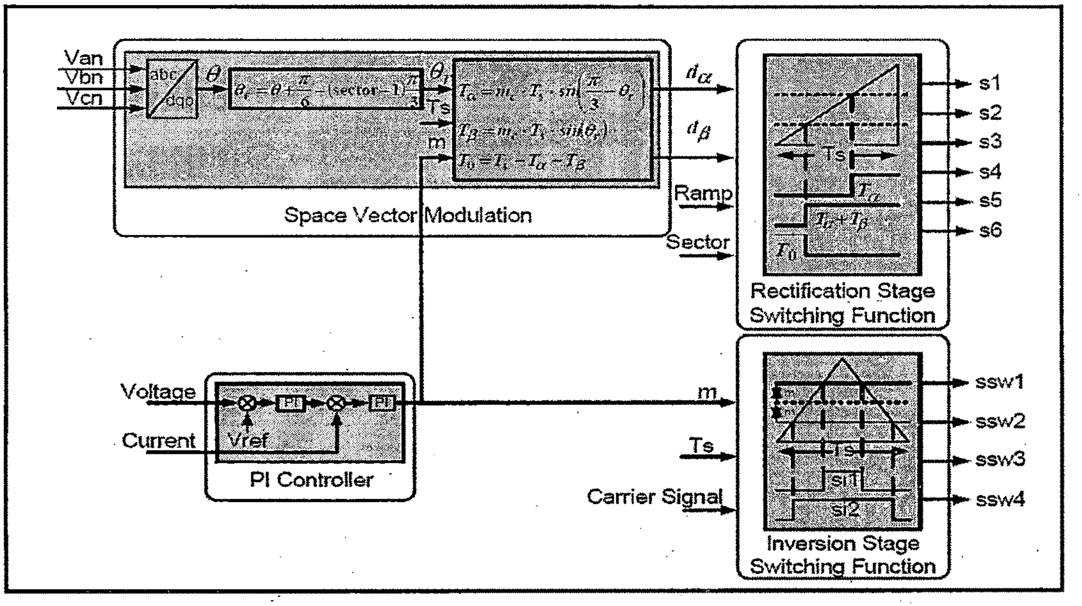

Fig. 6.8. Block diagram of the proposed matrix converter modulation.

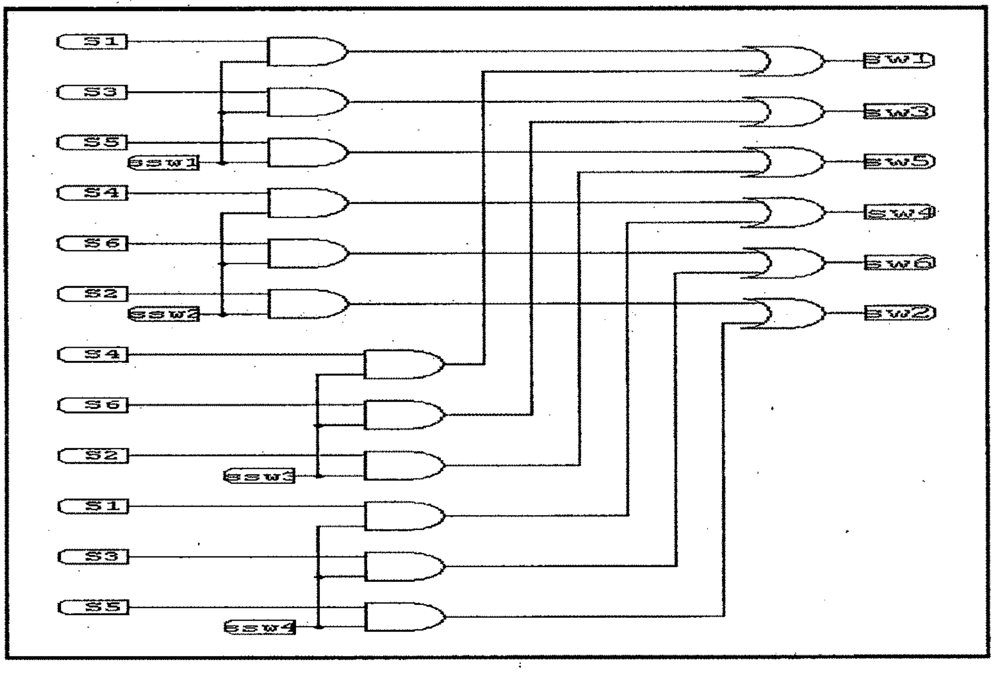

Fig. 6.9. Matrix converter switch gating signals generating through logic gates.

6.5 Design example

In this section a design example is presented. To facilitate calculation in per unit, the following base quantities are defined.

Output required power P_o = 2 kW

Output DC voltage V_{dc} = 48 V

Therefore output DC current I_{dc} = 41.67 A

Therefore the load impedance Z_l =1.152 Ω

Considering the above parameters as base values the input per unit line voltage is 4.33

The matrix converter output current I_o is given by,

$$\boxed{I_o = \frac{1}{N} * I_{dc}} \tag{6.22}$$

where N is the high frequency transformer turn ratio.

Select $N = 4$, $I_o = 0.25$ per-unit.

Neglecting conduction and switching losses, the utility line current can be expressed as:

$$\boxed{I_o = \frac{P_o}{\sqrt{3} * V_i}} \tag{6.23}$$

And the input current $I_a = 0.133$ per-unit.

The input and output specifications of the design are shown in Table 6.1.

Table 6.1. Design specifications of the proposed approach.

Design specifications Values	
Input line voltage (V_i)	208 V
Input frequency (f_i)	60 Hz
Switching frequency (f_{sw})	15 kHz
Output DC voltage (V_{dc})	48 V
Load power (P_o)	2.0 kW
Matrix converter module	1200V 6 modules of IGBTs-SK60GM123

6.6 Input filter design

High frequency current components in the input current of matrix converter can be filtered via a LC filter. The value of filter capacitor is selected by the following equation [28].

$$\boxed{C_f \approx \frac{2 * P}{3 * \omega_i * V_m^2}} \tag{6.24}$$

where P is the power rating, V_m is the peak of input voltage, and ω_i is angular input frequency.

The value of filter inductor is chosen by,

$$\boxed{L_f = \frac{1}{(2\pi f_c)^2 * C_f}} \tag{6.25}$$

where f_c is the cut-off frequency and is chosen to be lower than the switching frequency (15 kHz). With the parameter values given in this design example, and cutoff frequency is chosen to be 2.7 kHz:

Filter capacitance (C_F) = 82 µF.

Filter inductor (L_F) = 43 µH.

6.7 Simulation results

In this section simulation results of the proposed approach are discussed. Fig. 6.10 shows the three-phase input line voltages. Fig. 6.11 shows the high frequency output voltage of the matrix converter. Fig. 6.12 shows the 48 V DC output voltage.

Fig. 6.13 illustrates the performance of the proposed converter from utility perspective. It is clear for these results that input current is of high quality and is in phase with the input line to neutral voltage. Fig. 6.14 shows the variation of input current THD as a function of load.

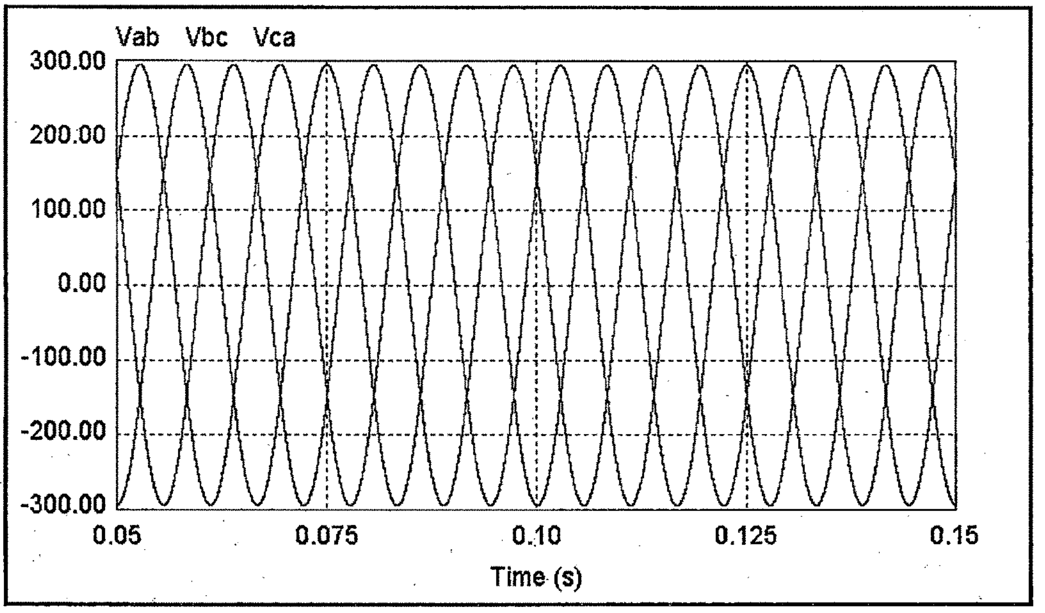

Fig. 6.10. The three-phase input voltages V_{ab}, V_{bc}, and V_{ca} : 208 V (rms) 60 Hz.

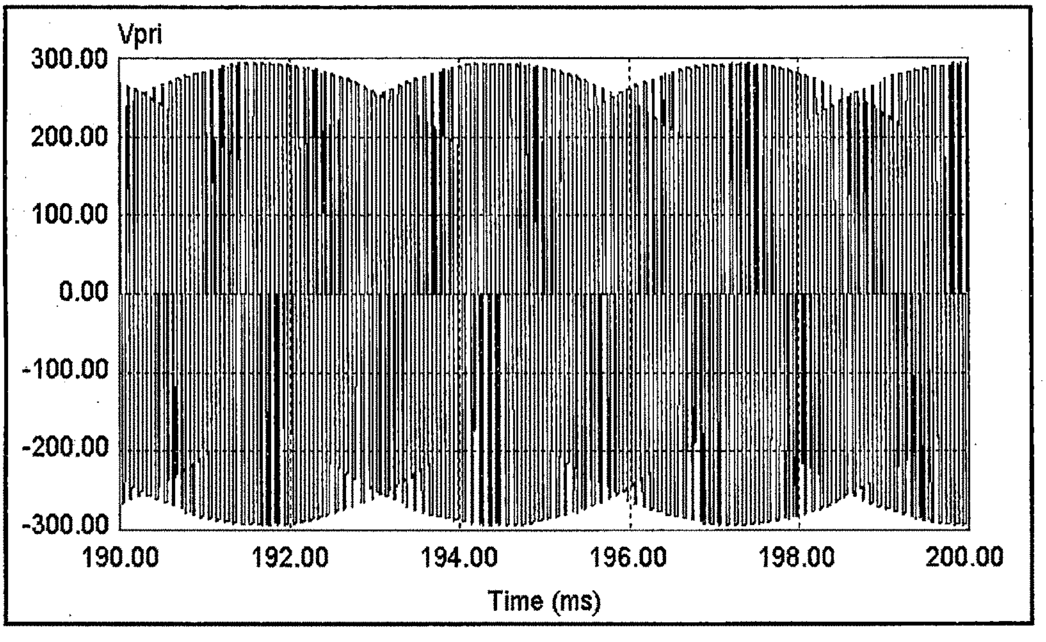

Fig. 6.11. High frequency output voltage *pri V* of the matrix converter.

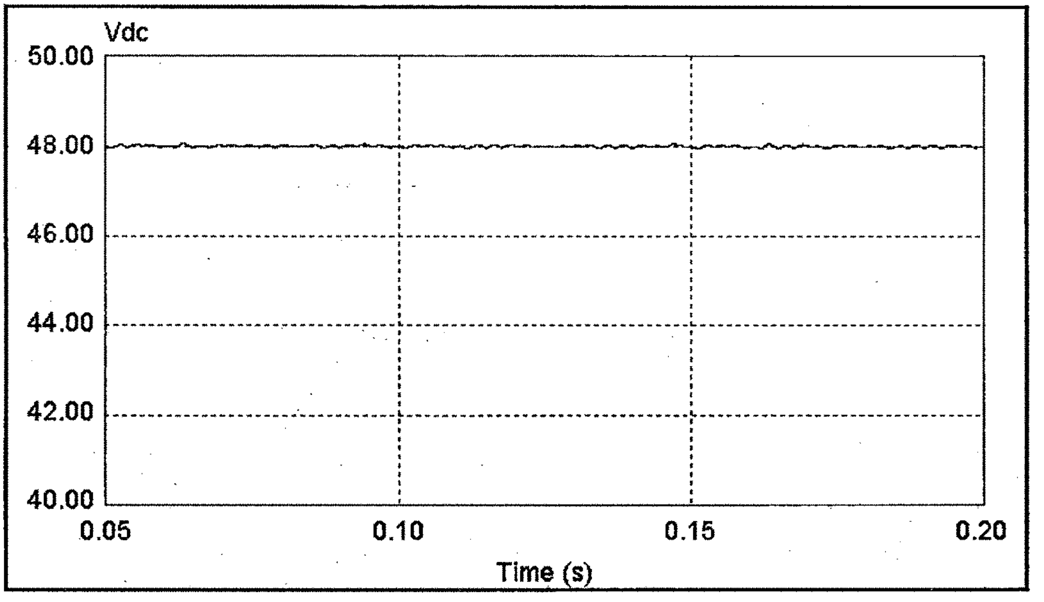

Fig. 6.12. Output DC voltage (48 V).

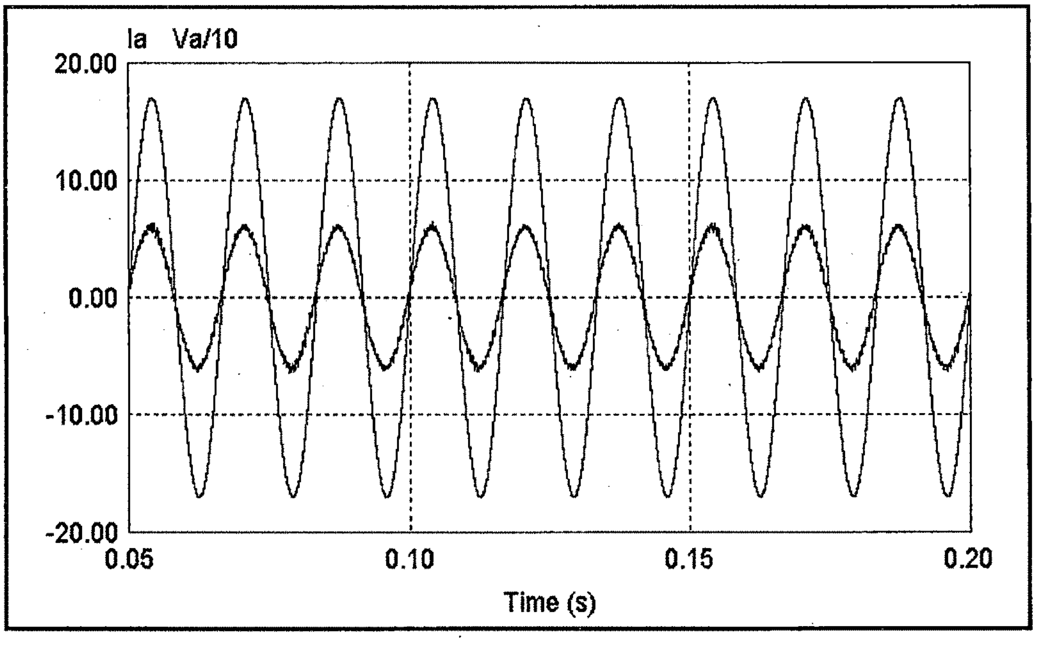

Fig. 6.13. Input line to neutral input voltage V_{an} and input current I_a.

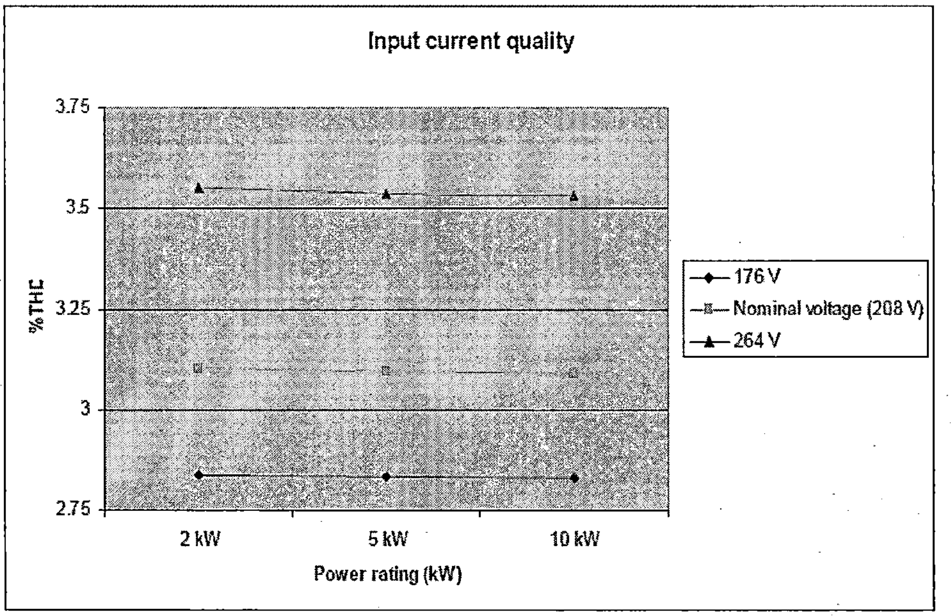

Fig. 6.14. THD percentage at different loads.

6.8 Experimental results

A laboratory prototype of the proposed digitally controlled switch mode power supply was constructed to meet the specifications detailed in section 4.5. A commercially available matrix converter module: SK 60GM123 from SEMIKRON was used. A digital signal processor (TMS320F2812) was used for generating PWM gating signals and performing closed loop functions. Fig. 6.15 shows the prototype matrix converter unit. The unit is connected to bridge rectifier, which consists of 4 fast-recovery diodes (60EPU02), and an output filter to produce power supply voltage of 48 V DC. Fig. 6.16 shows the input voltage V_{ab} , matrix converter output voltage (high frequency) *pri V* (connected to the transformer primary winding) and the transformer secondary voltage *sec V*. Fig. 6.17 shows the transformer primary and secondary voltages with expanded time scale. Fig. 6.18 shows the output DC voltage (48 V) and the load current. Fig. 6.19 shows the line to neutral voltage V_{an} and the line current I_a at 1.5 kW output power. It is clear that the input current is of high quality and unity power factor.

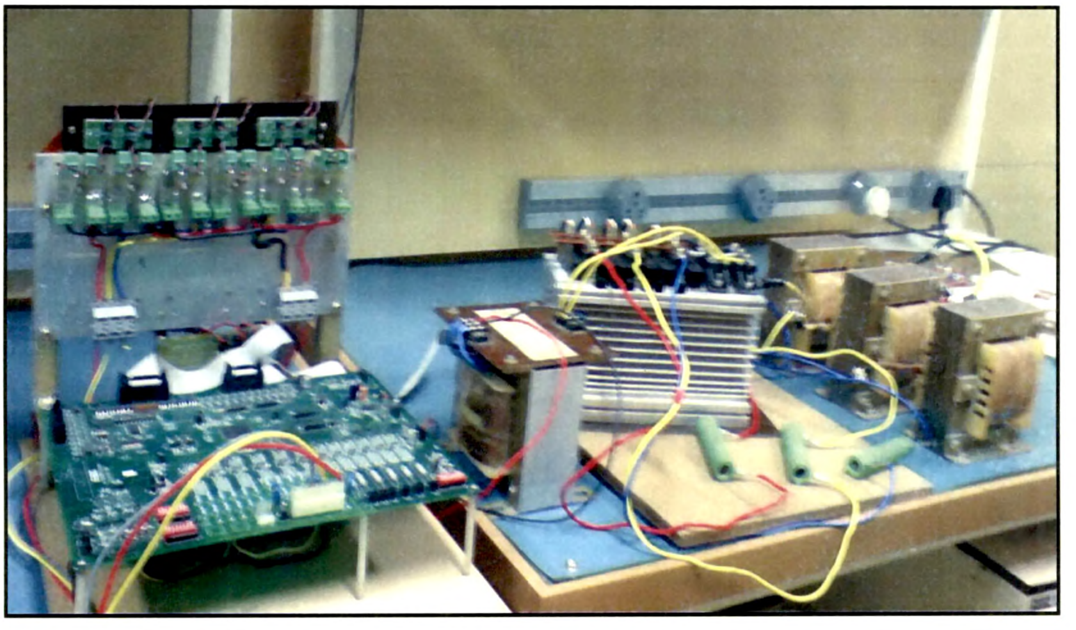

Fig. 6.15. Proposed matrix converter prototype.

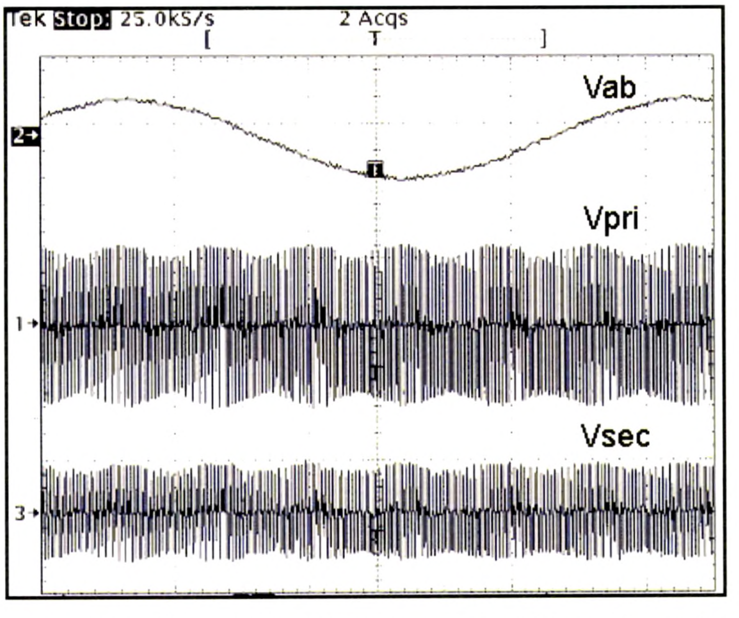

Fig. 6.16. Input voltage V_{ab}, matrix converter output voltage V_{pri}, and transformer secondary voltage V_{sec}.

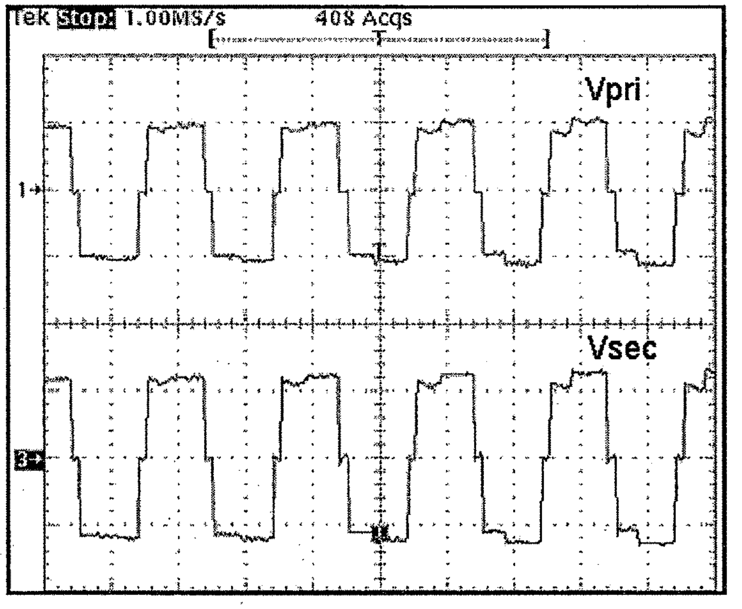

Fig. 6.17. Transformer primary *Vpri* and secondary voltages *Vsec*.

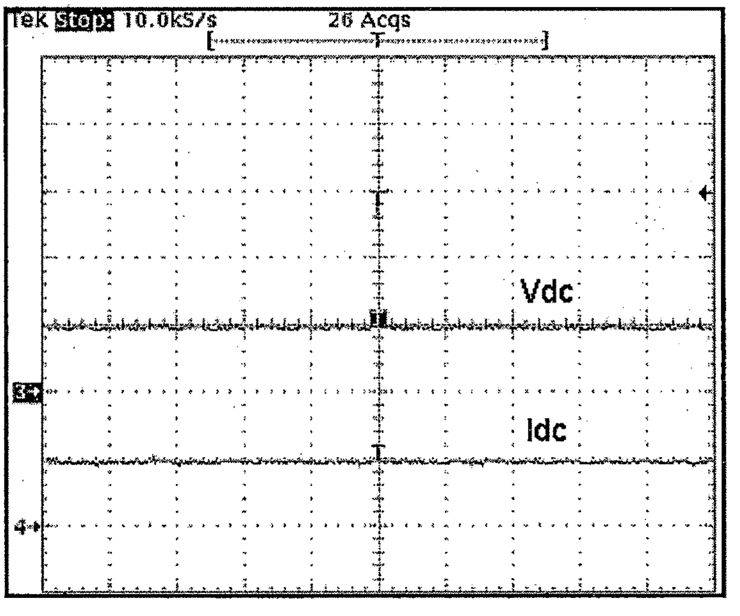

Fig. 6.18. Output DC voltage V_{dc} and load current I_{dc}.

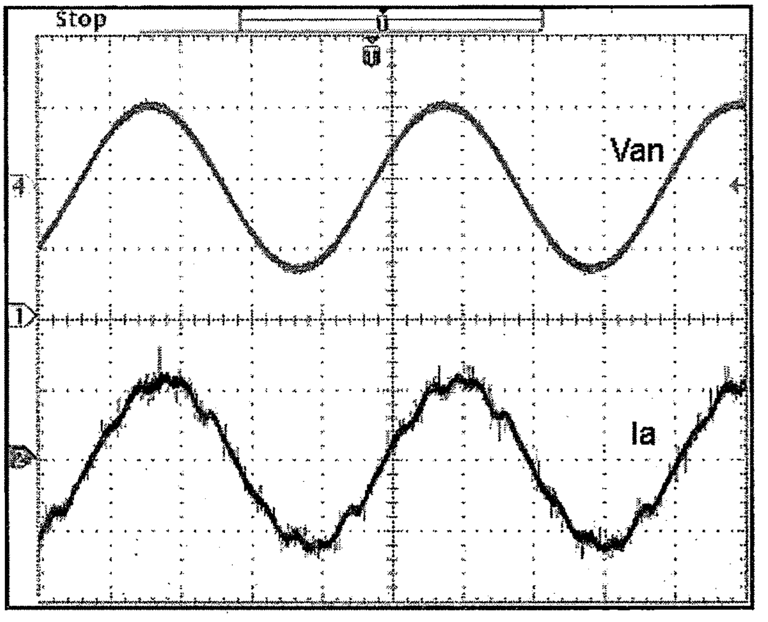

Fig. 6.19. Input line to neutral voltage *an V* and the input line current *a I* at 1.5 kW of output power.

The main factor, which has stimulated the use of renewable energy, is environmental protection. The cost disadvantage of renewable energy has resulted in numerous efforts to reduce its cost. For wind turbines, this has resulted in a continuously increasing rated power, as appears from Fig. 6.20 [67]. The objective of this chapter is to apply the proposed topology for variable frequency systems such as wind turbines and micro generators. Initially various electrical conversion systems used for wind turbines are studied and then the basic requirements for the drive system are discussed from some basic wind turbine characteristics. Next, the chapter describes the three classical generator systems with their strengths and weaknesses. Subsequently, the applied electric converters are shortly addressed. Finally, alternative generator systems and trends are discussed.

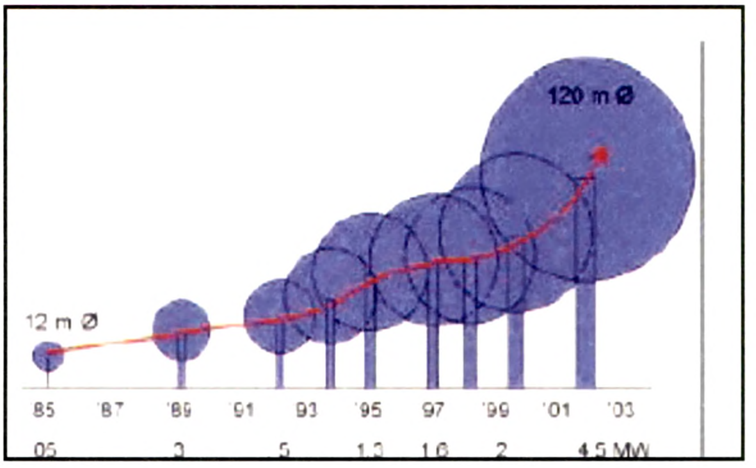

Fig 6.20 Development of power and size of wind turbines at market introduction

The power that can be captured from the wind with a wind energy converter with effective area *Ar* is given by equation 6.26.

$$\boxed{P = \frac{1}{2}\rho_{air} C_p A_r v_w^3} \tag{6.26}$$

where ρ_{air} is the air mass density [kg/m^3], v_w is the wind speed and C_p is the so-called power coefficient which depends on the specific design of the wind converter and its orientation to the wind direction. Its theoretical maximum value is 16/27 = 0.593 (Betz limit). For a wind turbine with given blades it can be shown that the power coefficient C_p basically depends only on the tip speed ratio λ, which equals the ratio of tip speed v_t [m/s] over wind speed v_w [m/s] and the so-called blade pitch angle θ [deg]. This pitch angle is defined as the angle between the cord of the blade and the plane of the wind rotor. So, for a wind rotor with radius *r*, (1) can be rewritten as:

$$\boxed{P = \frac{1}{2}\rho_{air} C_p (\lambda, \theta) \pi r^2 v_w^3} \tag{6.27}$$

6.9 Application of conventional Direct AC-AC converters for variable frequency wind turbine applications:

A vector controlled DFIM is an attractive solution for high performance, restricted speed range drives and energy generation applications. The typical connection scheme of DFIM is shown in Fig. 6.21. For limited speed variations around the synchronous speed of the induction machine, the power handed by the converter at rotor side is a small fraction (depending on slip) of the overall converted power. In variable speed drives during motor operating condition, the rotor slip power is regenerated to grid by the rotor power supply, resulting in efficient energy conversion. In variable speed energy generation applications, the asynchronous nature of the DFIM allows to produce constant-frequency electric power from a prime mover whose speed vary within a slip range (sub and super) of the DFIM synchronous speed. Variable-speed energy generation systems have several advantages when compared with fixed-speed synchronous and induction generation. In diesel engine and hydroelectric generation systems, it increases the energy efficiency up to 10%. In wind energy generation systems the adjustment of the shaft speed as a function of the wind speed permits higher energy capture by maximizing the turbine efficiency [11].

The fundamentals of DFIM vector control are presented in [73] and widely used in different developments [75]-[77]. In both motor and generator applications the DFIM is able to provide torque production together with stator side power factor control. If suitably controlled AC/AC converter is used to supply the rotor side of the DFIM, the power components of the overall system can be controlled with low harmonic distortion in the stator and rotor sides. Moreover, when the DFIM is used as a variable-speed drive, the slip power is regenerated during motor operating conditions by the converter to the line grid, resulting in highly efficient energy conversion.

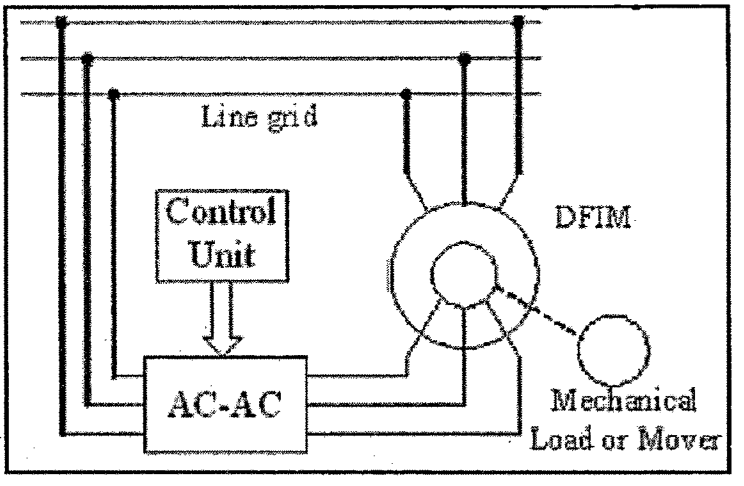

Fig 6.21 Schematic of connection of DFIM to the grid using AC-AC converter

The two approaches are possible to supply the DFIM rotor circuit: standard AC-DC-AC power converters having vector controlled input rectifier and matrix converter solutions. Some simulation results of MC application for DFIM control have been already reported in literature [78]-[80].

Let consider the DFIM model represented in terms of stator fluxes and rotor currents, then

$$\boxed{\begin{aligned} \dot{\omega} &= \frac{1}{J}(T - T_L) \\ \dot{\Psi}_{1d} &= -\alpha\Psi_{1d} + \omega_0\Psi_{1q} + \alpha L_m i_{2d} + u_{1d} \\ \dot{\Psi}_{1q} &= -\alpha\Psi_{1q} - \omega_0\Psi_{1d} + \alpha L_m i_{2q} + u_{1q} \end{aligned}} \tag{6.28}$$

$$\boxed{\begin{aligned} \dot{i}_{2d} &= -\gamma i_{2d} + \omega_2 i_{2q} + \alpha\beta\Psi_{1d} - \beta\omega\Psi_{1q} - \beta u_{1q} + \frac{1}{\sigma}u_{2d} \\ \dot{i}_{2q} &= -\gamma i_{2q} - \omega_2 i_{2d} + \alpha\beta\Psi_{1q} + \beta\omega\Psi_{1d} - \beta u_{1q} + \frac{1}{\sigma}u_{2q} \end{aligned}} \tag{6.29}$$

where $\boxed{\omega_2 = \omega_0 - \omega,\ \alpha = \frac{R_1}{L_1},\ \sigma = L_2\left(1 - \frac{L_m^2}{L_1 L_2}\right),\ \beta = \frac{L_m}{L_1\sigma},\ \gamma = \frac{R_2}{\sigma} + \alpha\beta L_m}$ (6.30)

The generated torque is equal to

$$\boxed{\begin{aligned} &T = \mu(\Psi_{1q} i_{2d} - \Psi_{1d} i_{2q}) \\ &where\ \mu = \frac{3}{2}\frac{L_m}{L_1} \end{aligned}} \quad (6.31)$$

The two main classes of DFIM technological application are considered. When DFIM is used as generator, the torque T_L in the first equation of (6.15) is a moving torque, generated by the primary mover, and stabilizing the mechanical system, whose general representation is

$$\boxed{\begin{aligned} &\dot{\omega} = \frac{1}{J}(T - T_L) \\ &T_L = k_{\omega m}\left(\omega - \omega_m^*\right) \end{aligned}} \quad (6.32)$$

where $k_{\omega m} > 0$ is the speed control gain of the primary mover and ω_m^* is the primary mover speed reference.

Electromagnetic torque T of the DFIM is the load torque for the mechanical system (6.19) of the primary energy converter. The main control objective of the DFIM operating as a generator is to produce the desired generated torque$T^*(t)$ independently of .In electrical drive applications the DFIM torque T is the moving torque that controls the speed of the mechanical system and is an external load torque T_L. The speed control objective is typically defined for such applications.

For both tasks the following output feedback control objectives are defined. Let consider the DFIM model, given by (6.17) and (6.19) and assume that:

- A1 - The stator voltage amplitude and frequency are constant (stator windings are directly connected to then line grid);

- A2 - Rotor position and speed, stator voltages and rotor currents are available from the measurements;
- A3 - DFIM parameters are known and constant.

Under these conditions it is required to design an output feedback control algorithm (rotor voltage vector $u_2^{(dr-qr)}$) which guarantees

1. For energy generation systems:
   - Asymptotic torque tracking under condition of stator flux field-orientation, i.e.

$$\boxed{\lim_{t\to\infty} \tilde{T} = 0, \tilde{T} = T - T^*} \tag{6.33}$$

   where $\tilde{T}$ is the torque error and T^* is a bounded torque reference trajectory with bounded first and second derivatives.
   - A smooth transient less connection of the stator windings to the line grid during the start-up procedure.
2. For electric drives application:
   - Asymptotic speed tracking together with the condition of asymptotic stator flux field-orientation under the condition of constant bounded load torque, i.e.

$$\boxed{\begin{array}{l}\lim\limits_{t\to\infty} \tilde{\omega} = 0 \\ \lim\limits_{t\to\infty} \left(u_1^T \Psi_1\right) = 0, \ \tilde{\omega} = \omega - \omega^*\end{array}} \tag{6.34}$$

   where $\tilde{\omega}$ is the speed tracking error and ω^* is a bounded speed reference trajectory with bounded first, second and third time derivatives.

This theory is basically used for designing the control of the nine-switch Direct AC-AC converter depending on the usage of the DFIM for generating or motoring action. The block diagram of the control that may be used with the mentioned AC-AC converter is shown in figure below

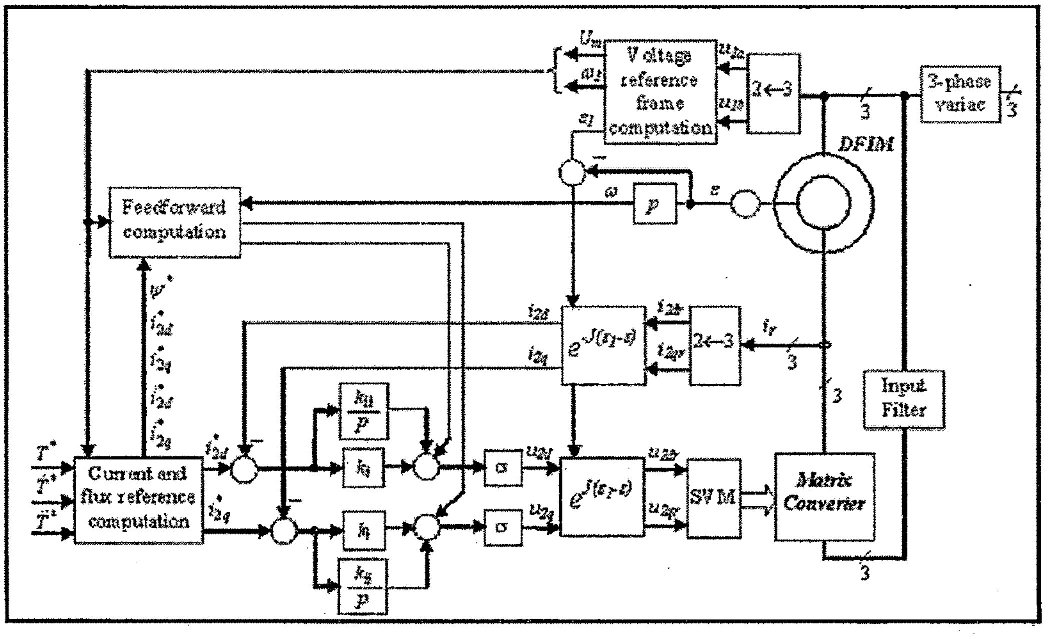

Fig 6.22 Block of Control of DFIM using Direct AC-AC converter

6.10 Implementation of proposed converter for control of DFIM for wind turbines

The power flow, illustrated in Fig.6.17, is used to describe the operating principle. Parameters used in this figure are described in Table 6.2. The mechanical power and the stator electrical power output are computed as follows:

$\boxed{\begin{array}{l} P_m = T\omega_r \\ P_s = T_L\omega_s \end{array}}$; where P_m is mechanical power and P_s is stator power

and for loss less generation of power the mechanical equation mentioned in Eqn 6.15 can be used. In steady state at fixed speed for a lossless generator is $T = T_L$ & $P_m = P_s + P_r$, where P_r is the rotor power.

From the above relation it follows:

$P_r = P_m - P_s = T\omega_r - T_L\omega_s = -(\frac{\omega_s - \omega_r}{\omega_s})P_s = -sP_s$, where s is defined as the slip of the generator. Generally the absolute value of slip is much lower than 1 and, consequently, P_r is only a fraction of P_s. Since T_m is positive for power generation and since ω_s is positive and constant for a constant frequency grid voltage, the sign of Pr is a function of the slip sign.

Table 6.2: Parameter Definitions

P_m	Mechanical power captured by the wind turbine and transmitted to the rotor
P_s, Q_s	Stator active and reactive power output
P_r, Q_r	Rotor active and reactive power output
P_{gc}, Q_{gc}	C_{grid} active and reactive power output
T	Mechanical torque applied to rotor
T_L	Electromagnetic torque applied to the rotor by the generator
ω_r	Rotational speed of rotor
ω_s	Rotational speed of the magnetic flux in the air gap of the generator. This synchronous speed is proportional to the frequency of the grid voltage and to the number of generator poles.
J	Combined rotor and wind turbine moment of inertia

P_r is positive for negative slip (speed greater than synchronous speed) and it is negative for positive slip (speed lower than synchronous speed). For super synchronous speed operation, P_r is transmitted to DC bus capacitor and tends to raise the DC voltage. For sub-synchronous speed operation, P_r is taken out of DC bus capacitor and tends to decrease the DC voltage. C_{grid} is used to generate or absorb the power P_{gc} in order to keep the DC voltage constant. In steady-state for a lossless AC-AC converter P_{gc} is equal to P_r and the speed of the wind turbine is determined by the power Pr absorbed or generated by C_{rotor}. The power control will be explained below.

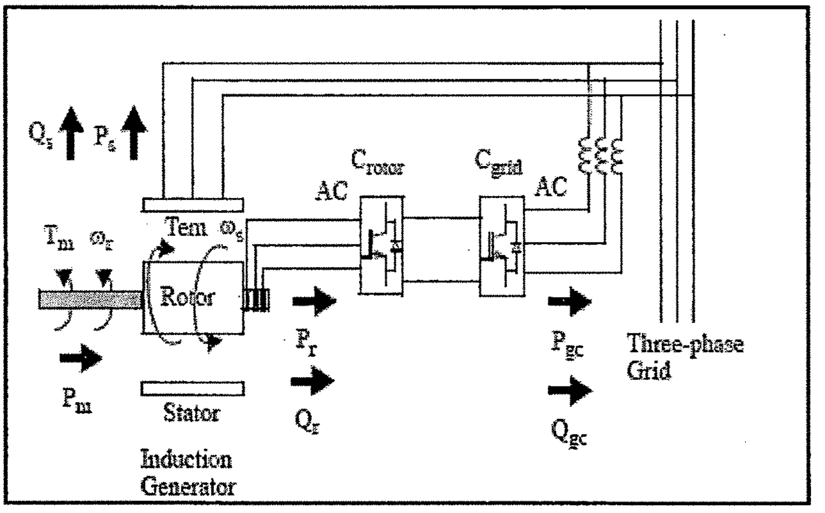

Fig 6.23 Active and Reactive power flow in DFIG

The phase-sequence of the AC voltage generated by C_{rotor} is positive for sub-synchronous speed and negative for super synchronous speed. The frequency of this voltage is equal to the product of the grid frequency and the absolute value of the slip. C_{rotor} and C_{grid} have the capability for generating or absorbing reactive power and could be used to control the reactive power or the voltage at the grid terminals.

6.10.1 C_{rotor} control system

The rotor-side converter is used to control the wind turbine output power and the voltage measured at the grid terminals. The power is controlled in order to follow a pre-defined power-speed characteristic, named tracking characteristic. This characteristic is illustrated by the ABCD curve in Fig. 6.23 superimposed on the mechanical power characteristics of the turbine obtained at different wind speeds. The actual speed of the turbine ωr is measured and the corresponding mechanical power of the tracking characteristic is used as the reference power for the power control loop. The tracking characteristic is defined by four points viz. A, B, C and D. From zero speed to speed of point A the reference power is zero. Between point A and point B the tracking characteristic is a straight line. Between point B and point C the tracking characteristic is the locus of the maximum power of the turbine (maxima of the turbine power v/s turbine speed curves). The tracking characteristic is a straight line from point C and point D. The power at point D is one per unit (1 p.u.). Beyond point D the reference power is a constant equal to one per unit (1 p.u.).

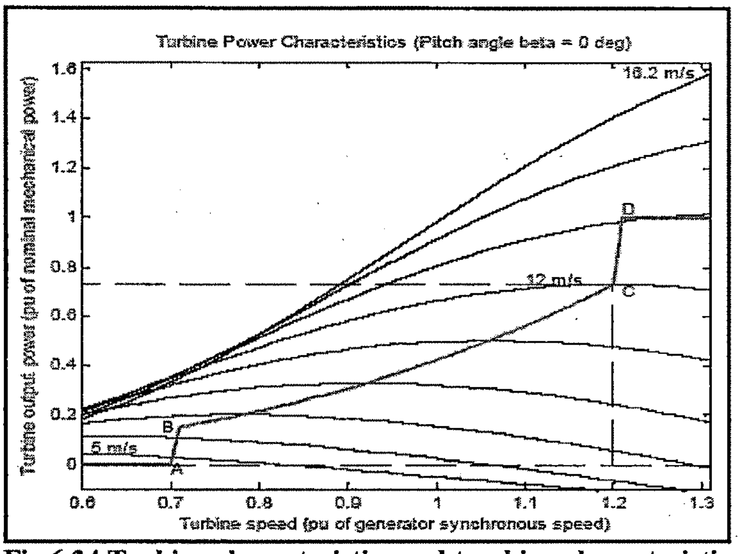

Fig 6.24 Turbine characteristics and tracking characteristic

For the rotor-side controller the d-axis of the rotating reference frame used for d-q transformation is aligned with air-gap flux. The actual electrical output power, measured at the grid terminals of the wind turbine, is added to the total power losses (mechanical and electrical) and is compared with the reference power obtained from the tracking characteristic. A Proportional-Integral (PI) regulator is used to reduce the power error to zero. The output of this regulator is the reference rotor current I_{qr_ref} that must be injected in the rotor by converter C_{rotor}. This is the current component that produces the electromagnetic torque T_L. The actual I_{qr} component is compared to I_{qr_ref} and the error is reduced to zero by a current regulator (PI). The output of this current controller is the voltage V_{qr} generated by C_{rotor}. The current regulator is assisted by feed forward terms, which predict V_{qr}. The voltage at grid terminals is controlled by the reactive power generated or absorbed by the converter C_{rotor}. The reactive power is exchanged between C_{rotor} and the grid, through the generator. In the exchange process the generator absorbs reactive power to supply its mutual and leakage inductances. The excess of reactive power is sent to the grid or to C_{rotor}. The generic control loop is illustrated in Fig. 6.25b. The wind turbine control implements the V-I characteristic illustrated in Fig. 6.26.

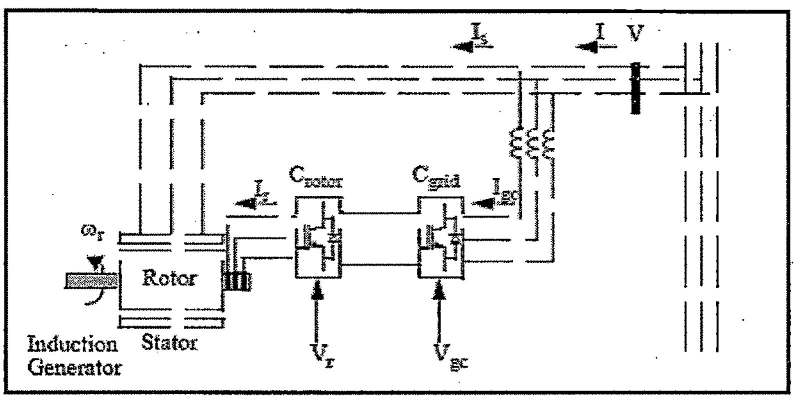

a) Rotor and Grid side converters

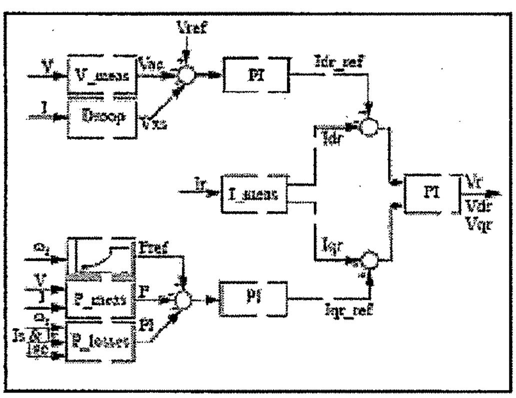

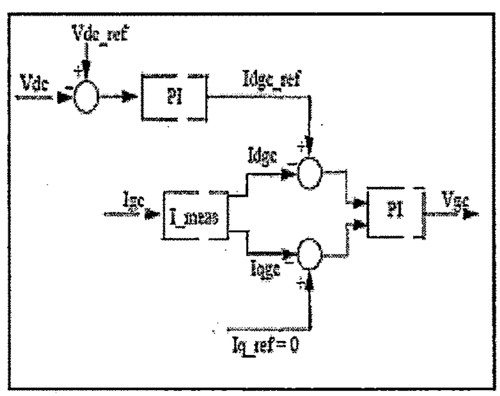

b) Rotor side controller **c) Grid side controller**

Fig. 6.25. Rotor-side and grid-side converters and control systems

As long as the reactive current stays within the maximum current values (-Imax, Imax) imposed by the converter rating, the voltage is regulated at the reference voltage V_{ref}. A voltage droop is used for the V-I characteristic shown on Fig. 6.26 (3% at maximum reactive power output).

6.10.2 C_{grid} control system

The converter C_{grid} is used to regulate the voltage of the DC bus capacitor. The control system is illustrated in Fig. 6.19c.

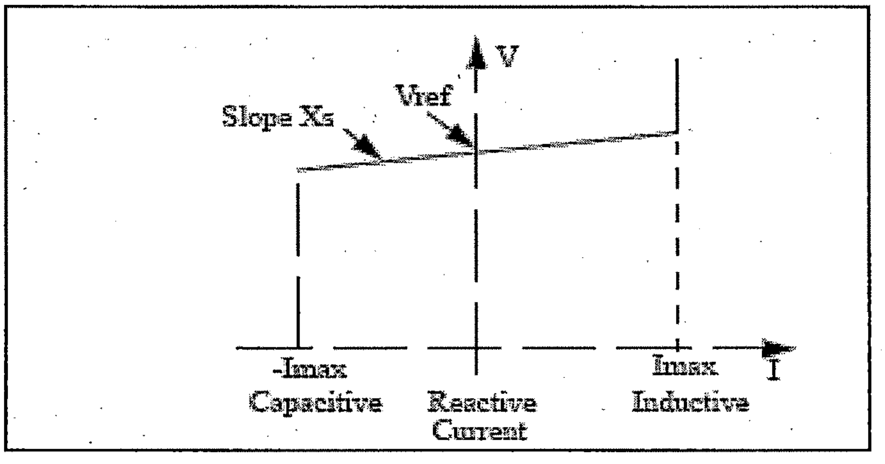

Fig 6.26 V-I characteristics of a Wind Turbine

For the grid-side controller the d-axis of the rotating reference frame used for d-q transformation is aligned with the phase A of grid voltage. This controller consists of:

1- A measurement system measuring the d and q components of AC currents to be controlled as well as the DC voltage V_{dc}

2- An outer regulation loop consisting of a DC voltage regulator. The output of the DC voltage regulator is the reference current I_{dgc_ref} for the current regulator (I_{dgc} = current in phase with grid voltage which controls active power flow).

3- An inner current regulation loop consisting of a current regulator. The current regulator controls the magnitude and phase of the voltage generated by converter C_{grid} (V_{gc}) from the I_{dgc_ref} produced by the DC voltage regulator and specified I_{q_ref} reference. The current regulator is assisted by feed forward terms, which predict the C_{grid} output voltage.

6.11 Conclusion

In this initial part of this chapter a digitally controlled switch mode power supply based on matrix converter for telecommunication applications has been shown. The proposed space vector PWM method has been shown to yield high quality input current for varying load conditions. Experimental results on a 2 kW prototype have demonstrated the feasibility of a direct AC to AC matrix converter in telecommunication power supplies.

In the later part of the chapter, an effort is made to use the proposed converter to control a double fed induction generator used for wind application. Theoretical analysis and its feasibility study is carried out. A part of control algorithm for this application is briefly explained.